Multi-Parameter POD for Industrial Applications The Influence of the Material Attenuation as an Example

Mato PAVLOVIC, Rainer BOEHM, Christina MÜLLER, BAM, Berlin, Germany
Ulf RONNETEG, SKB, Oskarshamn, Sweden

Abstract. The multi-parameter reliability analysis of the inspection data from the thick copper specimens[5)] gathered with the phased array ultrasonic system, showed that not only the size of the flaw influence the probability of detection (POD), as it is assumed in conventional signal response analysis[6)]. The influence of the size, depth and orientation of the flaw on the POD was investigated. The attenuation of the ultrasonic waves in material was included in calculation, but considered constant.

In this paper, it is demonstrated that the attenuation in copper can drastically vary within the specimen and has significant influence on defect detection. Therefore, the calculation with variable (local) coefficient of attenuation in material α is performed. The POD curve dependent on material attenuation coefficient is shown, emphasizing its practical application.

INTRODUCTION

The nuclear power industry has the responsibility for management and disposal of all radioactive waste from its plants. International consensus is that deep geological disposal on land is the most appropriate means for isolating high-level waste from the environment[1)]. The method to manage nuclear waste being investigated by SKB and Posiva is called KBS-3 method[2)]. It calls for the spent nuclear fuel to be encapsulated in copper. The copper canisters will be deposited in the bedrock, embedded in clay, at a depth of about 500 meters.

The canisters are approximately five meters long and have a diameter of over one meter. The outer shell is made of copper due to its high resistance to corrosion. It is five centimetres thick and should prevent contact of the content of the canister with the environment. Inner part made of cast iron is designed to withstand mechanical loads imposed on the canister.

NDT of all parts of the canister will be carried out to ensure that no critical defect is present in material. From many available NDT methods, the advanced ultrasonic (UT) phased array system is selected as a primary method for the inspection.

Inspection systems, even the most advanced, when applied at the extreme of capability for finding small flaws, will not detect all flaws of the same size. It is known from the

practice that even repeated inspections of the same flaw will not always detect it, meaning that the measurements are not consistent due to the noise, measurement errors, and inconsistency of setups. This is why the concept of reliability is introduced.

The "Non-Destructive Testing Reliability Project" is a joint project between Swedish Nuclear Fuel and Waste Management Co (SKB); Posiva Oy, a Finnish expert organisation responsible for the final disposal of spent nuclear fuel and German Federal Institute for Material Research and Testing (BAM). The project is a subpart of the total risk assessment of the final repository[3)4)].

Building on the previous work[5)], addition of the material attenuation coefficient as a parameter in multi-parameter reliability analysis is shown in this paper.

AMPLITUDE DISTRIBUTION

The intensity of the ultrasonic wave typically changes as the wave propagates. The cause of this change in intensity can be attributed to two sources. The change due to the beam spreading or the apparent attenuation[7)] is caused by geometrical spreading of the sound beam. In natural materials, the sound effect additionally weakens due to effects present in materials.

Amplitude change due to the beam spreading

In ideal materials, the reduction of amplitude intensity of the sphere wave will be inversely proportional to the distance traveled. In phased array ultrasonics, by using different excitation time of individual elements, the sound field can be formed by varying the interference conditions, i.e. the focused beam can be generated. Example of such beam profile is shown in Figure 1 as calculated by the ultrasonic simulation software developed in BAM, division VIII.4 Acoustic and Electric Methods. The software uses the point source synthesis (PSS) method taking into account the elastodynamic behaviour at the material boundaries[4)].

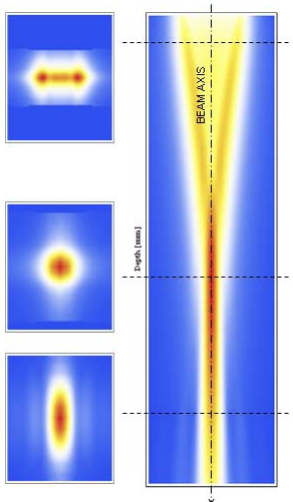

Figure 1. *Focused ultrasonic beam*

Depending on the distance from the probe and focal laws used, the amplitude of the beam will change. Figure 2 shows the dependence of the amplitude on the axis of the beam with respect to the distance from the probe.

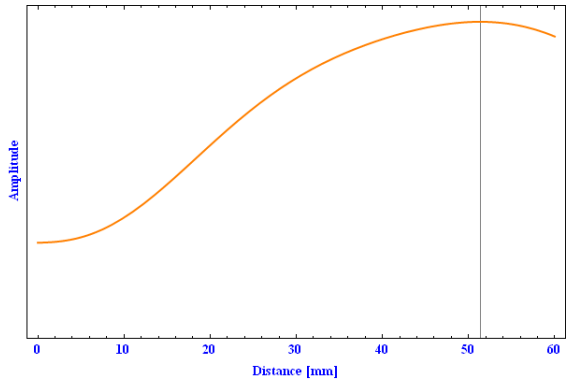

Figure 2. *Change of amplitude on the axis of the beam (see Figure 1) with respect to the distance from the probe with indicated focal point*

As it can be seen, the amplitude is not diminishing with the distance but has a maximum value at the focal point and after that decreases. The focal point is the distance at which the beam has highest intensity and this will have direct influence on increased POD of the flaws in that region.

Attenuation in material

The presence of the natural material on the path of the sound wave propagation will cause attenuation of its intensity. Origins of this attenuation are the scattering and absorption that happen in the material. It is mainly dependent upon the damping capacity and scattering from the grain boundary in the material. Figure 3 shows microscopic images of copper specimens with different grain sizes[11]. The start grain size was 60 μm resulted from hot rolling. This grain size was modified with variable hot pressing reduction from 20% to 61%. It is easy to comprehend why absorption and scattering of the sound wave in those specimens were quite different. Both the average grain size and the distribution influence the attenuation.

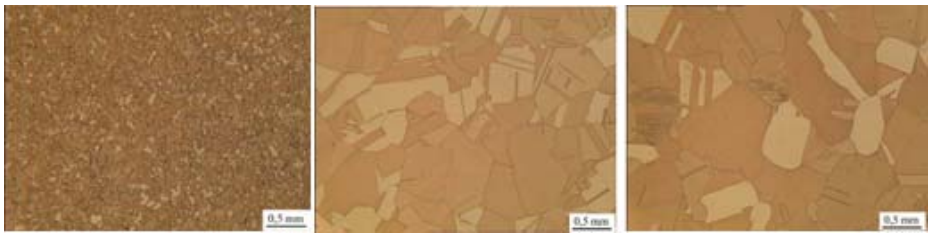

Figure 3. *Microscopic image of copper specimens with different grain sizes*

From the theory[9], the attenuation of the amplitude A follows inverse exponential law (Figure 4):

$$A = A_0 * e^{-\alpha * z} \qquad (1)$$

where A_0 is the unattenuated amplitude at some initial location, A is the attenuated amplitude after the wave has travelled a distance z from the initial location. The quantity α is the attenuation coefficient.

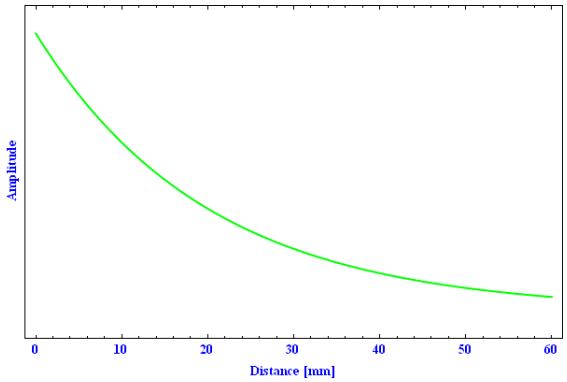

Figure 4. *Inverse exponential law of attenuation in material*

Overall change of amplitude

Overall change of amplitude of the sound wave is a product of the change due to the beam spreading and of the attenuation in material:

$$A = A_{BS}(\vec{r}) * A_M(\alpha, z) \qquad (2)$$

where A is the overall amplitude, A_{BS} the change in amplitude due to the beam spreading dependent on the position $\vec{r}$ and A_M the attenuation of the amplitude due to the presence of material, dependent on the coefficient of attenuation α and distance z. When all three functions are plotted in one diagram (Figure 5), a couple of interesting effects can be observed. The presence of material will reduce the amplitude of the beam formed by the probe. The higher the attenuation in material, the amplitude will be more reduced. The second interesting effect is that the attenuation in material will shift the point of maximum amplitude (focal point) closer to the probe. That means that the focal point, which is set using the focal laws, will shift depending on the attenuation in material. Again, the higher the attenuation in material, the focal point will move more toward the probe.

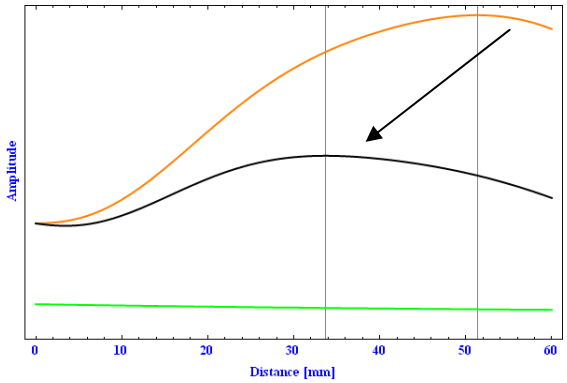

Figure 5. *Change of amplitude due to the beam spreading with indicated maximum amplitude (orange curve), attenuation in material (green curve) and overall change of amplitude with indicated maximum amplitude (black curve)*

EXPERIMENT

Test specimens

To investigate the influence of the material attenuation on the detection capability of the phased array UT NDT system, flat bottom holes (FBH) were manufactured in two copper specimens. Full factorial design with two factors (diameter and depth) was used. The selection of levels of factors was based on the previous experience of the sensitivity of the NDT system used. The FBHs were manufactured with diameters ranging from 1 to 3 mm in step of 0.5 mm and in depths from 6 to 60 mm with three repetitions of each FBH, making the total of 150 FBHs. Position of the FBHs was randomized within the block. The FBHs were manufactured in two steps in a high-precision milling machine. First standard drills were used to obtain the depth and diameter of the holes and secondly flat-bottom shaped drills were used to achieve a smooth flat surface. By the use of an EDM machine, the depth and diameter was verified to be within ±0.02 mm. The test specimens are shown in Figure 6.

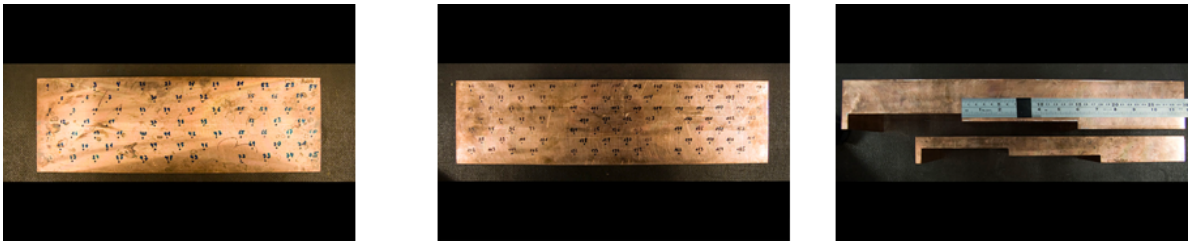

SPECIMEN 1 *SPECIMEN 2* *SIDE VIEW*

Figure 6. *Copper test specimens*

Phased array ultrasonic system

The inspection of the copper specimen was performed with UT phased array system. Probe frequency was 5 MHz. The technique used was immersion in water with 30 mm water path. The beam had a normal incidence. During transmission, 16 elements were used focused at the 55 mm depth. In receiving mode, 16 elements were used with dynamic depth focusing.

RESULTS

Backwall echo

C-scans of the aquired data show great variations in the amplitude of the backwall echoes (BE). This variation is caused by the different local properties of the material causing different local attenuation of the sound wave. In Figure 7 it can be seen that the BE can vary from location to location more than three times in magnitude.

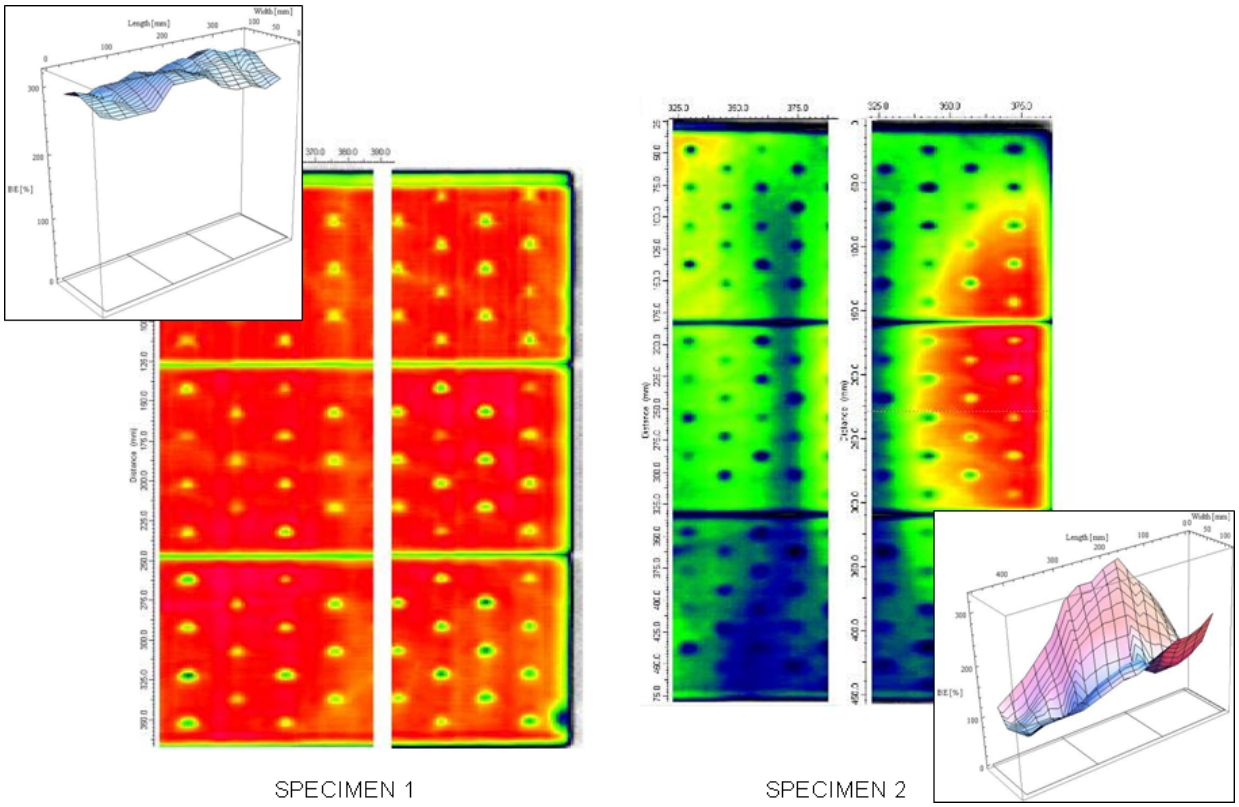

Figure 7. *Backwall echo amplitudes in two test specimens (C-scans and 3-D plots)*

Reflection amplitude of the FBH

Reflection amplitude of each FBH was measured exactly at the position of the FBH and results are shown in Figure 8. Numbers in diagram represent the diameter of the measured FBH amplitude. As already mentioned, there are three FBHs with the same diameter and in the same depth. The line with corresponding colour connects the mean values of those three measurements. In homogenous material, it is expected that the line has a shape similar to the overall attenuation curve from Figure 5. It can be seen that it is not the case and observe some curious behaviour. Sometimes the reflection amplitude of the FBH with smaller diameter is higher than the reflection amplitude of the FBH with larger diameter, although they are in the same depth. Obviously, the FBH with smaller diameter is in the region of lower attenuation than the FBH with larger diameter. As it can be seen, the attenuation is changing depending on the position x and y. To investigate attenuation change in z direction, side scans of the test specimens were also performed as illustrated in Figure 9. From the C-scan from side inspection, it can be seen that the change of attenuation in depth direction z is relatively small compared to the change in x and y directions. It can be assumed:

$$\alpha = \alpha(x, y) \qquad (4)$$

meaning that the material coefficient α changes depending on the position x and y of the specimen, but it is constant with depth z. To account for this local change of attenuation, the model calculation has to be carried out with local coefficient of attenuation, α_i.

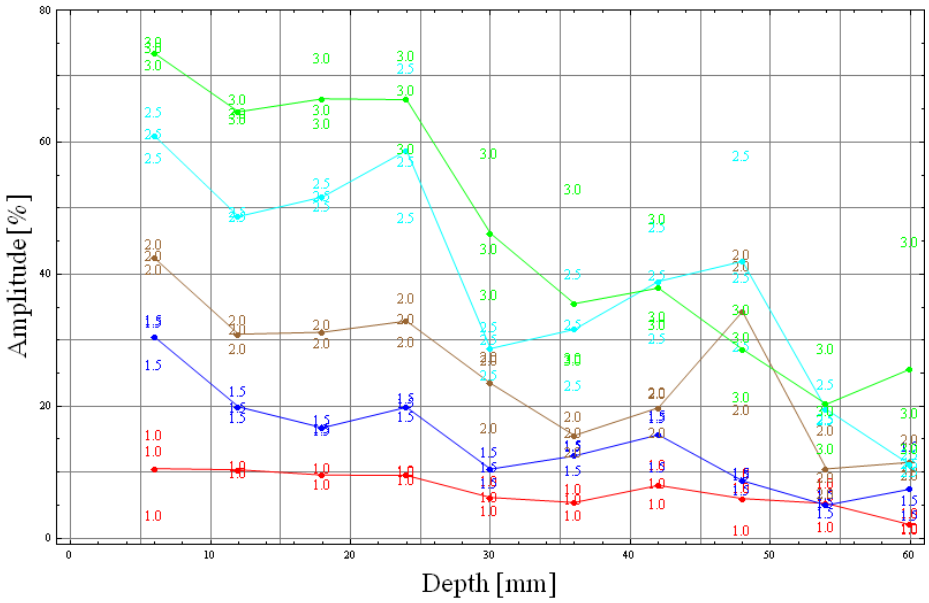

Figure 8. *Reflection amplitude of individual FBHs*

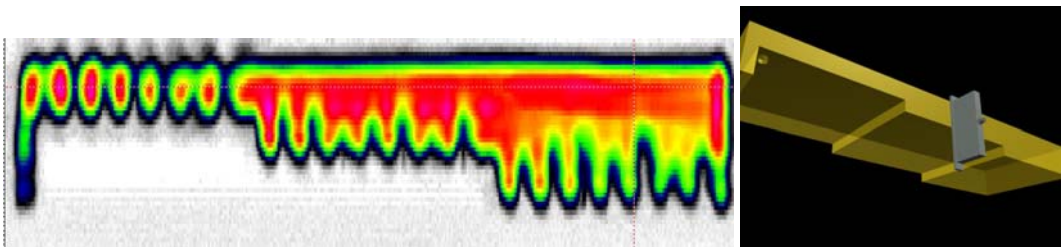

Figure 9. *C-scan (left) from the side inspection of the test specimen, schematically shown on the right*

Local coefficient of attenuation in material

Amplitudes that are measured contain influence of both the attenuation due to the beam spread and due to the material attenuation. To scale the model to the measured values with the actual equipment used, the scale factor and the local coefficient of attenuation have to be determined. To estimate it, the BE measurements from the thin, 15 mm thick part of the test specimen are used, where the impulse was long enough to record four backwall echoes (Figure 10). The measurement of the backwall echoes was carried out on four different locations and the results are shown in Figure 11 left. The lost of amplitude is shown in percentage of amplitude. Measured values converted to decibels and expressed as a lost of amplitude from the first backwall echo shows Figure 11 right.

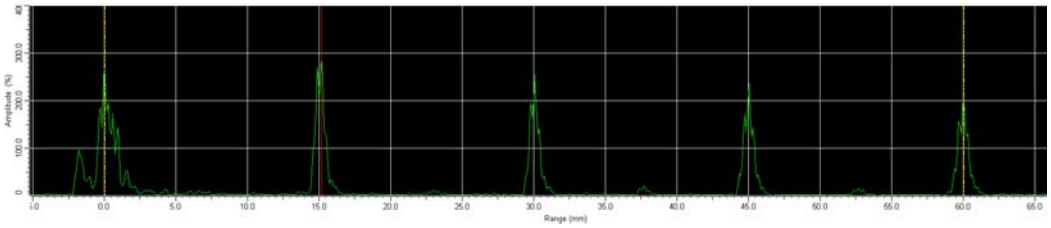

Figure 10. *A-scan of multiple backwall echoes*

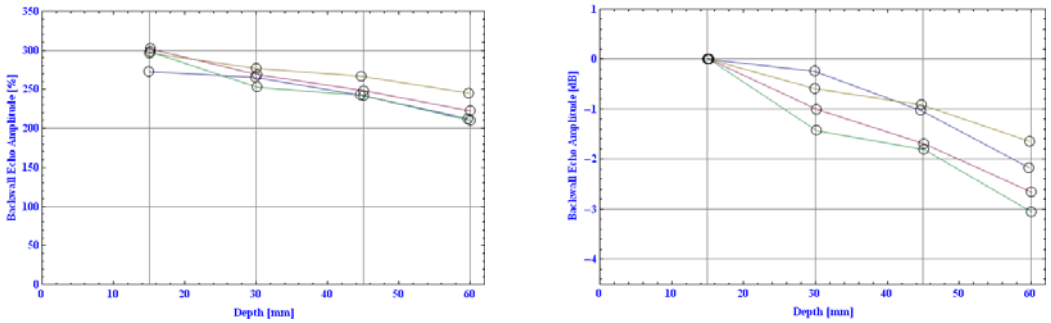

Figure 11. *Measurement of multiple backwall echoes, percentage of amplitude (left) and lost in decibels of the first echo (right)*

As expected, the lost of amplitude is different from location to location. Measured values contain both the influence of the beam spread and attenuation in material. Values without the influence of the beam spreading are shown in Figure 12 left whilst the same expressed as lost of amplitude of the first echo in decibels is shown in Figure 12 right. Comparing Figure 11 with Figure 12 it can be seen that the lost of amplitude only due to the material attenuation is higher than one actually measured. This is achieved with the beam focusing of the phased array probe. From these measurements, the mean scale factor is calculated. It is assumed that it is same for all FBHs.

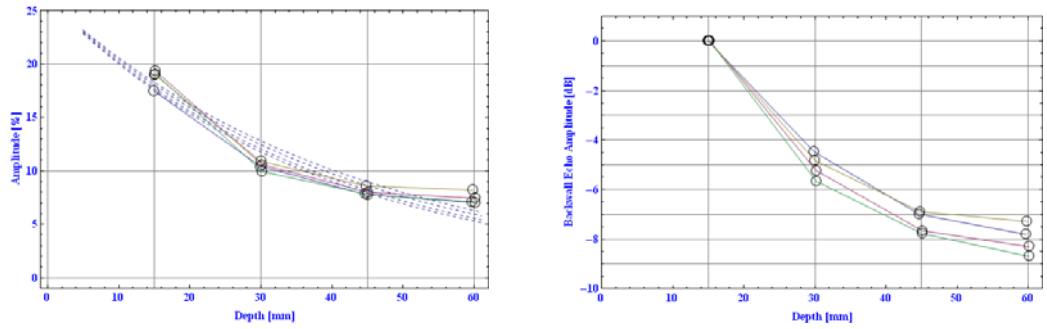

Figure 12. *Measurement of the amplitude of multiple backwall echoes, without the influence of the beam spreading with fitted inverse exponential functions (left); lost of amplitude in decibels of the first echo (right)*

Knowing the scale factor, the local coefficient of attenuation α_i for each FBH is determined from the Equation (1) using the amplitude of the local BE. The measured values plotted against model values with linear regression line are plotted in Figure 13. The left diagram shows model calculated with one, constant α for the whole specimen and the diagram on the right calculation with local α_i. It can be seen that the scatter of the data with local α_i is smaller than for the model with constant α. The regression line of the model with local α_i is in addition closer to the ideal, 45° line.

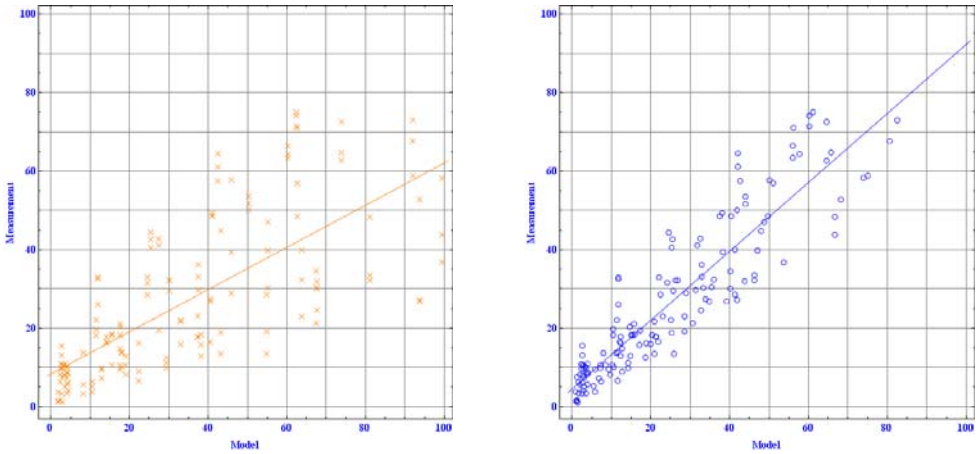

Figure 13. *Comparison of the models with constant and variable coefficient of attenuation α_i*

Probability of detection

The next step is to calculate the POD curve with lower 95% confidence band of the FBHs with respect to the multi-parameter *a*. Using the local noise level in the region of the FBH and setting the decision threshold to 3 signal-to-noise ratio (SNR) the multi-parameter POD curve is calculated[5)10)]. From this curve, it is possible to calculate the POD curves with respect to individual parameters. Figure 14 shows the POD curve with lower 95% confidence band of the FBH with diameter 1.5 mm in material with attenuation coefficient 0.35 dB/mm, with respect to depth.

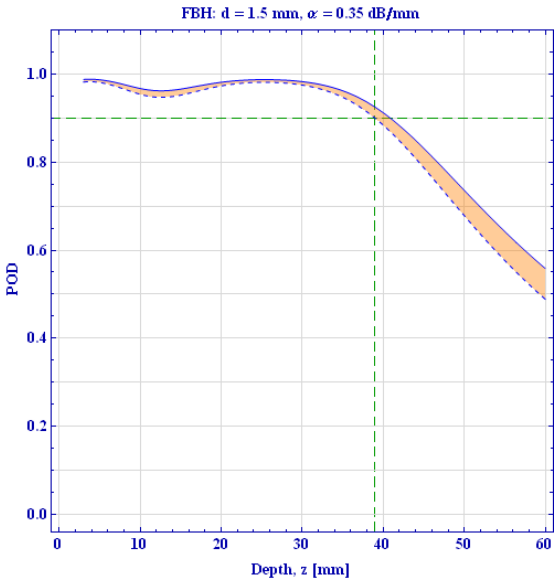

Figure 14. *POD curve of the FBH with diameter 1.5 mm in material with attenuation coefficient α = 0.04Np/mm, with respect to depth*

This curve is similar to the conventional POD curve and it is used in the same manner. The point where the lower 95% confidence band is below the 90% probability, the NDT system is not sufficient for the defect detection. In example shown, the NDT system will be acceptable for the detection of the defect in material up to almost 40 mm depth. In Figure 15 for clarity are only plotted the lower 95% confidence bands for materials with different attenuation coefficient. The diagram can be used to compare the POD of the flaw in materials with different attenuation. It is important to notice that the diagram can be used only for inspection configuration presented here because the attenuation coefficient is of the

material only, while overall amplitude will change depending on the focal laws used with the probe.

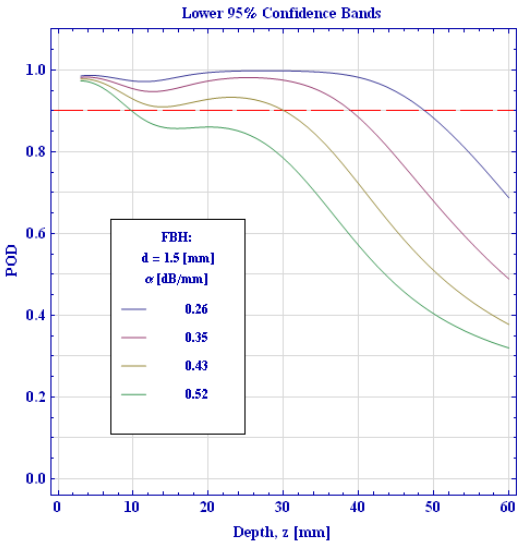

Figure 15. *Lower 95% confidence bands of the FBH with 1.5 mm diameter for materials with different attenuations with respect to depth*

CONCLUSIONS

Investigation has shown that the attenuation in copper material used for canisters can vary considerably. Influence of the attenuation on the POD of the flaws is not to be neglected. Provided POD curves, which use the material coefficient as parameter, give information if the NDT system is capable to detect certain defect with sufficient probability. These curves can be easily used in practice as acceptance criteria for quality of manufactured copper parts. Maximal grain size, which is directly proportional to the ultrasonic attenuation in material, can be set as a requirement for manufacturing. By measuring the BE in the part, it can be assured that all critical defects can be detected with sufficient probability with used NDT system.

The shortcoming of the presented method is that the attenuation coefficient is estimated with the UT measurement, same way as the inspection itself is performed. Some other way to estimate the attenuation coefficient should be investigated in the future, possibly as suggested in[7)].

It is known that the attenuation coefficient is highly dependant on frequency. At this point, the investigation was performed only with the 5 MHz probe that is currently used by the SKB. Intention is to continue investigation including the inspection frequency as a parameter.

REFERENCES

1) NEA Group of Experts, “Objectives, Concepts and Strategies for the Management of Radioactive Waste Arising from Nuclear Power Programmes”, OECD/NEA, Paris, 1977.
2) SKB, RD&D Programme, *Programme for research, development and demonstration of methods for the management and disposal of nuclear waste, TR-07-12.* SKB AB., 2007
3) Ronneteg U, Müller C, Pavlovic M, “Reliability in NDT of Canister for the Swedish Spent Nuclear Fuel”, *4th European-American Workshop on Reliability of NDE*, Berlin, 2009

4) Pitkänen J, Bertovic M, Müller C, Pavlovic M, Salonen T, "NDT Reliability in Risk Minimization during Manufacturing and Welding of Spent Nuclear Fuel Disposal Components - A Realistic Tool for Reliable Inspections", *4th European-American Workshop on Reliability of NDE,* Berlin, 2009

5) Pavlovic M, Takahashi K, Müller C, Boehm R and Ronneteg U, "NDT reliability – Final report, Reliability in non-destructive testing (NDT) of the canister components", *SKB Technical report R-08-129*, Swedish Nuclear Fuel and Waste Management Co., 2008.

6) Berens A P, "NDE Reliability Data Analysis", *ASM Metals Handbook, Volume 17, 9th Edition: Nondestructive Evaluation and Quality Control*, Materials Park, Ohio, ASM International, 1988

7) Stepinski T and Engholm M, "Inspection of copper canisters for spent nuclear fuel by means of ultrasound Copper characterization, FSW monitoring with acoustic emission and ultrasonic imaging", *SKB Technical report TR-09-28*, Swedish Nuclear Fuel and Waste Management Co., 2009.

8) Boehm R, Erhard A, Rehfeldt T, „Einfluss fokussierter Schallfelder auf das Reflexionsverhalten von Testfehlern", in Proc. *DGZfP-Jahrestagung*, Mainz, 2003

9) Krautkrämer J and Krautkrämer H, *Werkstoffprüfung mit Ultraschall*, Berlin, Heidelberg, New York, Springer Verlag, 1980

10) Pavlovic M, Takahashi K, Ronneteg U, Pitkänen J, Müller C, "Multi-Parameter Influence on the Response of the Flaw to the Phased Array Ultrasonic NDT System. The Volume POD.", *4th European-American Workshop on Reliability of NDE,* Berlin, 2009

11) Pitkänen J, Arnold W, Hirsekorn S, "The Effect of Grain Size on the Defect Detectability in Copper Components in Ultrasonic Testing", *6th International Conference on NDE in Relation to Structural integrity for Nuclear and Pressurized Components*, Budapest, 2007